

Cavity Ring-Down Spectroscopy as a Detector for Liquid Chromatography

Kate L. Snyder and Richard N. Zare*

Department of Chemistry, Stanford University, Stanford, California 94305-5080

We have demonstrated the use of cavity ring-down spectroscopy (CRDS) as a detector for high performance liquid chromatography (HPLC). For this use, we have designed and implemented a Brewster's angle flow cell such that cavity ring-down spectroscopy can be performed on microliter volumes of liquids. The system exhibits a linear dynamic range of 3 orders of magnitude (30 nM to 30 μ M quinalizarin at 470 nm) for static measurements and 2 orders of magnitude (0.5 μ M to 50 μ M) for HPLC measurements. For the static measurements, the baseline noise is 2.8×10^{-6} AU rms and 1.0×10^{-5} AU peak-to-peak, and for the HPLC separations, it is 3.2×10^{-6} AU rms and 1.3×10^{-5} AU peak-to-peak. The baseline noise is determined after the data are smoothed by an 11-point boxcar average. The peak areas detected from HPLC separations are reproducible to within 2–3%. The HPLC mass detection limit for a molecule with $\epsilon = 9 \times 10^3 \text{ M}^{-1} \text{ cm}^{-1}$ in a 300- μ m path length cell (illuminated volume, 0.5 μ L) is reported as 2.5×10^{-8} g/mL. These results were obtained using a simple pulsed CRDS system and are comparable to, if not better than, a high-quality commercial UV–vis absorption detector for the same path length.

High performance liquid chromatography (HPLC) is the analytical method of choice for separation, purification, and detection in numerous areas of research and industry. Of the many detection methods for liquid chromatography, the most often employed is UV–vis absorption, because it is nearly universal and is reasonably sensitive (5×10^{-8} g/mL).¹ A fundamental limitation of traditional UV–vis absorption detectors is the fact that a small difference between two relatively large signals is being measured. As a result, the sensitivity of absorption detectors is largely dependent on the ability to measure I_0 and I well enough to obtain a small $\Delta I/I$ value (currently on the order of 5×10^{-5}). Other factors influencing sensitivity are sample path length and the photon flux through the system. For a shot-noise-limited detector, the signal-to-noise ratio will increase as the square root of the incident light intensity.² Intense light sources, such as lasers, would be desirable to increase the number of photons striking the detector, but lasers tend to suffer from intensity fluctuations, reducing their advantage. Thus, commercial absorption detectors

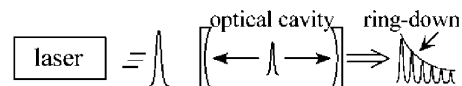


Figure 1. Schematic diagram of a simple pulsed CRDS experiment.

use stable lamps (deuterium, xenon, or tungsten) as the light source instead of lasers. Additionally, matched photodiodes are used in some instruments to compensate for the small power fluctuations of the lamp by ratioing the outputs of the reference beam and the sample beam for each measurement. This detection scheme allows for the small $\Delta I/I$ value obtained by commercial instruments.

Insensitivity to light intensity fluctuations is an attribute of cavity ring-down spectroscopy (CRDS), a relatively new approach to absorption measurements.^{3–5} CRDS in its simplest form consists of a pulsed laser as the light source, an optical cavity formed by two highly reflective mirrors facing one another, and a detector. A laser pulse enters the cavity through the back of the first mirror and bounces back and forth inside the cavity, leaking out a small amount at each bounce. Depending on its time resolution, the detector can resolve either each individual pulse exiting the cavity or the envelope of its exponential decay, as illustrated in Figure 1.

The rate constant for the exponential decay of light intensity depends on all losses of light within the optical cavity. These losses include fixed losses from the optics (such as the mirrors and objects placed inside the cavity) and losses caused by absorption and scattering of the analyte and the solvent. The time constant, τ , of the exponential decay of light intensity is related to the concentration of the absorbing medium by

$$\tau = \frac{t_{rt}}{2[\delta_m + \delta_c + \alpha l]} \quad (1)$$

Here, t_{rt} is the round-trip time for light in the cavity, given by $2L/c$, where L is the cavity length and c is the speed of light; δ_m includes all mirror losses (typically approximated as $1 - R$, where R is the mirror reflectivity); δ_c includes all other cavity losses not including absorption by the analyte of interest; and αl is the Beer's law absorption of the analyte of interest, where α is the per-pass absorption coefficient of the analyte and l is the sample path

* To whom correspondence should be addressed. E-mail: zare@stanford.edu.

(1) Scott, R. P. W. *Chromatographic Detectors*; Chromatographic Science Series; Marcel Dekker: New York, 1996; Vol. 73, p 186.
 (2) Ingle, J. D., Jr.; Crouch, S. R. *Spectrochemical Analysis*; Prentice Hall: Englewood Cliffs, NJ, 1988.

(3) O'Keefe, A.; Deacon, D. A. G. *Rev. Sci. Instrum.* **1988**, *59*, 2544–2551.
 (4) O'Keefe, A.; Scherer, J. J.; Cooksy, A. L.; Sheeks, R.; Heath, J.; Saykally, R. *J. Chem. Phys. Lett.* **1990**, *172*, 215–218.
 (5) Zalicki, P.; Zare, R. N. *J. Chem. Phys.* **1995**, *102*, 2708–2717.

length. The absorption coefficient, α , is related to its log base 10 analogue by the expression $\alpha = 2.303\epsilon C$, in which ϵ is the molar extinction coefficient, C is the concentration, and 2.303 is a constant to convert from natural log to log base 10. The absorption coefficient is determined from the ring-down time constants with and without the absorber present,

$$\alpha = \frac{t_{rt}}{2l} \left(\frac{\tau_0 - \tau}{\tau_0 \tau} \right) \quad (2)$$

where τ is the ring-down time constant with the absorber present and τ_0 is the ring-down time constant with only the solvent present. CRDS is insensitive to intensity fluctuations because the absorption coefficient is determined by measuring the rates of decay of the light exiting the cavity, which is not dependent on the initial light intensity (provided that the intensity is within the linear range of the detector). CRDS also has a gain in sensitivity resulting from its multipass nature.

The minimum detectable absorption coefficient per pass is determined by⁶

$$\alpha_{\min} = \sqrt{2} \frac{L(\sigma_{\tau}/\bar{\tau}_0)}{l\bar{\tau}_0} \quad (3)$$

where σ_{τ} is the standard deviation of the mean value of the ring-down time, $\bar{\tau}_0$, without the analyte present. In the shot noise limit, $\sigma_{\tau}/\bar{\tau}_0$ is determined by the reciprocal of the square root of the number of photons incident on the detector. If shot noise is not the limiting factor, then to minimize $\sigma_{\tau}/\bar{\tau}_0$ and to maximize $\bar{\tau}_0$, the optical losses within the cavity should be reduced as much as possible. In gas-phase CRDS, this task is typically not a problem because the only optical losses are from the cavity mirrors. Up to the point that low light throughput does not decrease the signal-to-noise (S/N) ratio by elevating the shot noise, the mirror reflectivities can be increased to achieve a lower detection limit. In the solid and liquid phases, however, the sample must be placed within the optical cavity without it or its container, introducing significant losses into the system. In the solid phase, this task has been achieved by depositing a thin film directly onto the mirror surface,^{7,8} placing a thin film in the cavity, either perpendicular to the beam such that embedded cavities are formed^{9,10} or at Brewster's angle^{11,12} or by evanescent wave CRDS. Pipino et al.^{13–16} developed evanescent wave CRDS in which the sample of interest is contained on the back of a prism placed inside a ring-down cavity, where it makes contact with the evanescent wave

formed at the total-internal-reflection (TIR) surface of the prism. This technique has been applied to liquids as well for the study of the silica-water interface.¹⁷ Although excellent for examining surface properties, evanescent wave CRDS is not useful for measuring the absorption properties of the bulk solution.

The application of CRDS to the measurement of the bulk absorption of liquids presents a special challenge. For instance, inserting a standard UV–vis cuvette inside a ring-down cavity would introduce a 4% reflection loss at each surface of the cuvette, resulting in a ring-down lifetime that is too short to measure well. This problem has been countered in various ways. Hallock et al.¹⁸ demonstrated liquid CRDS by filling the entire ring-down cavity with the liquid of interest, allowing it to come into contact with the mirrors. This approach has been applied to kinetic studies¹⁹ using volumes on the order of milliliters. This method is not suitable for measuring small volumes of liquid, owing to the short ring-down lifetimes resulting from the necessarily close mirror separation. Xu et al.²⁰ inserted two standard UV–vis cuvettes into a ring-down cavity at Brewster's angle to try to minimize the reflection losses at each interface. Xu's technique is rather limited because the refractive index of the liquid sample must be close to that of the fused-silica cuvette ($n = 1.46$), which for liquids is not very common. In addition, the scattering and absorption loss of the large amount of solvent used in both Xu's and Hallock's instruments resulted in very small ring-down lifetimes. For all of these techniques, the ring-down time constant ranged from 100 to 400 ns, where detector and electronic noise prevail, and none have been applied as a detector for analytical separations.

Our approach is to use a liquid flow cell that has been designed so that light strikes each surface at the correct Brewster's angle for the specific interface (air \rightarrow fused silica, fused silica \rightarrow liquid, liquid \rightarrow fused silica, fused silica \rightarrow air). With the appropriate polarization of light, the reflections are minimized, allowing the light to pass through the cell hundreds of times, which results in a relatively long ring-down time constant. Brewster's angle, defined by $\tan \theta_B = n_t/n_i$, where θ_B is Brewster's angle, n_t is the index of refraction of the medium in which light is transmitted, and n_i is the index of refraction of the medium in which light is incident, is the angle at which light plane-polarized parallel to the plane of incidence has theoretically no reflection loss. Because of the imperfect nature of most surfaces, a 0% reflection loss is not realized. Nonetheless, losses are sufficiently reduced to obtain a ring-down lifetime that is readily measured with little error. With pure water in a 300- μm optical path length Brewster's angle flow cell, a τ of 2.5 μs has been achieved in a 1-meter cavity. Furthermore, the flow cell has been successfully coupled to HPLC so that analytes are detected by on-line absorption using CRDS.

In what follows, we describe the experimental setup, present results from both static measurements and chromatographic separations, and compare the results to a state-of-the-art commercial HPLC absorption detection system. We discuss the performance characteristics of the present on-line CRDS detector

(6) Romanini, D.; Lehmann, K. K. *J. Chem. Phys.* **1993**, *99*, 6287–6301.
 (7) Curran, R. M.; Crook, T. M.; Zook, J. D. *Mater. Res. Soc. Symp. Proc.* **1988**, *105*, 175–180.
 (8) Kleine, D.; Lauterbach, J.; Kleinemanns, K.; Hering, P. *Appl. Phys. B* **2001**, *72*, 249–252.
 (9) Engeln, R.; Helden, G. v.; Roij, A. J. A. v.; Meijer, G. *J. Chem. Phys.* **1999**, *110*, 2732–2733.
 (10) Logunov, S. L. *Appl. Opt.* **2001**, *40*, 1570–1573.
 (11) Paldus, B. A.; Harb, C.; Zare, R. N.; Meijer, G. U.S. patent US6452680.
 (12) Muir, R. N.; Alexander, A. J. *Phys. Chem. Chem. Phys.* **2003**, *5*, 1279–1283.
 (13) Pipino, A. C. R.; Hudgens, J. W.; Huie, R. E. *Rev. Sci. Instrum.* **1997**, *68*, 2978–2989.
 (14) Pipino, A. C. R.; Hudgens, J. W.; Huie, R. E. *Chem. Phys. Lett.* **1997**, *280*, 104–112.
 (15) Pipino, A. C. R. *Phys. Rev. Lett.* **1999**, *83*, 3093–3096.
 (16) Pipino, A. C. R. *Appl. Opt.* **2000**, *39*, 1449–1453.

(17) Shaw, A. M.; Hannon, T. E.; Li, F.; Zare, R. N. Submitted.
 (18) Hallock, A. J.; Berman, E. S. F.; Zare, R. N. *Anal. Chem.* **2002**, *74*, 1741–1743.
 (19) Hallock, A. J.; Berman, E. S. F.; Zare, R. N. *J. Am. Chem. Soc.* **2003**, *125*, 1158–1159.
 (20) Xu, S.; Sha, G.; Xie, J. *Rev. Sci. Instrum.* **2002**, *73*, 255–258.

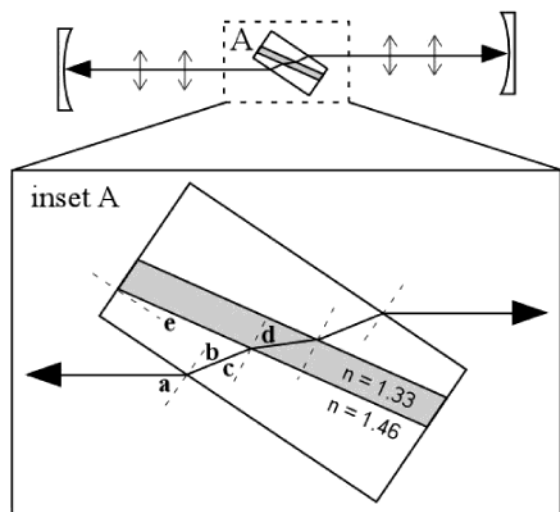


Figure 2. Schematic diagram of Brewster's angle flow cell inside a ring-down cavity. The vertical double arrows indicate the light is polarized parallel to the plane of incidence of the cell. The inset shows an expanded view of the cell. With a material index of 1.46 for fused silica and a liquid index of 1.33 for water, the optimal wedge angle, e , is 7.9° . With this configuration, the cell should be tilted so that the angle of light incidence, a , is 55.6° . The light refracts through the cell, hitting each surface at the appropriate angle for minimum reflection. These Brewster's angles are $b = 34.4^\circ$, $c = 42.3^\circ$, and $d = 47.7^\circ$.

and assess its possible use as an alternative detector for more miniaturized chromatographic separations.

EXPERIMENTAL SECTION

Apparatus. The ring-down cavity consists of a linear arrangement of two high-reflectivity mirrors ($R = 0.9993$ at 470 nm, Los Gatos Research, Sunnyvale, CA) separated by 1 m. The Brewster's angle flow cell is situated at the center of the cavity. The light source is a Nd:YAG laser-pumped OPO (Spectra Physics MOPO, Mountain View, CA) oscillating at 10 Hz with a pulse duration of 10 ns. A Hamamatsu R4692 photomultiplier tube (PMT) is used for detection. Data collected from a 500 MHz LeCroy LT342 oscilloscope are transferred to and analyzed on a PC.

The Brewster's angle flow cell was constructed as per our specifications by Hellma Cells, Inc., (Plainview, NY). The cell is constructed of UV-grade fused silica and polished to $15/3 \times 0.063$ as per DIN standard 58170, part 54 (similar to ISO 10110-7, Method 1). The flow thickness is $200 \mu\text{m}$, but the optical path length is $\sim 300 \mu\text{m}$ because of light passage at Brewster's angle. The illuminated volume is $0.5 \mu\text{L}$, though the total cell volume is $10 \mu\text{L}$ because of initial engineering constraints. This dead volume will be removed in future versions of the flow cell. A schematic of the flow cell inside a ring-down cavity is shown in Figure 2.

The beam is displaced a few millimeters in the transverse direction by the tilt angle of the cell. To offset this displacement, the back mirror is placed on a translation stage and aligned with the cell in place. Alignment is quite simple and remarkably robust. Once aligned, the system remains stable for weeks with no adjustments.

The acceptance angle for the Brewster condition inside an optical cavity is relatively broad ($\pm 0.5^\circ$)²¹ because cavity losses are negligible unless greater than the mirror losses. For this

reason, small changes in refractive index, such as those caused by absorbing species or temperature changes, do not alter significantly the ring-down time constant. Additionally, the optimum angles for the flow cell are very similar for a range of indices. Thus, a wide variety of solvents and analytes can be measured using the same flow cell. For instance, though this flow cell is specifically designed for a liquid with $n = 1.33$ (nominally water), it has been used for solvents ranging from methanol, $n \sim 1.33$, to acetone, $n \sim 1.36$, with no more than a couple hundred nanosecond difference in τ (a change of $\sim 10\%$) from one solvent to the other. The differing ring-down rates result from losses induced by changes in the index of refraction and the absorption of the particular solvent. Because the ring-down time is slightly different for each solvent, this system may require calibration for gradient separations.

Data Analysis. Each ring-down trace (collected at 10 Hz) is transferred from the oscilloscope to the computer and fit to an exponential function using the Levenberg–Marquardt method. For the HPLC measurements, the time constant, τ , extracted from this fit versus time gives a chromatogram. Approximately every 500–1000 laser shots, an extreme outlier point is obtained resulting from the misfiring of the laser, which is expected as per the laser's specifications. These points are confirmed as outliers using the statistical z test and discarded. The data are then converted to absorbance units using eq 2 and the fact that $AU = \alpha I / 2.303$. Once the chromatogram is obtained in terms of AU, the data are smoothed by an 11-point boxcar average using IGOR Pro software (WaveMetrics).

HPLC. Chromatography was performed with a homemade system consisting of a Beckman model 110A HPLC pump, a Valco Cheminert 6-port injection valve, and an Agilent Zorbax Eclipse XDB-C18 guard column and analytical column. The column contained end-capped C_{18} , $5\text{-}\mu\text{m}$ particles, and had dimensions $150 \text{ mm} \times 4.6 \text{ mm}$ i.d. The separation was carried out using an isocratic mobile phase of methanol/5% acetic acid in water (80:20 v/v) with a pH of 3.6. The flow rate of the mobile phase was 1.0 mL/min. Injections were made using the analytical-sized injector equipped with a $20\text{-}\mu\text{L}$ sample loop. Peaks were detected at 470 nm, a compromise of the visible wavelengths for maximum absorption of the five compounds separated.

Reagents. Alizarin (1,2-dihydroxyanthraquinone), purpurin (1,2,4-trihydroxyanthraquinone), quinalizarin (1,2,5,8-tetrahydroxyanthraquinone), emodin (6-methyl-1,3,8-trihydroxyanthraquinone), and quinizarin (1,4-dihydroxyanthraquinone) were purchased from Sigma-Aldrich (St. Louis, MO) and used without further purification. These molecules are members of the anthraquinone family, and their structures are shown in Table 1.

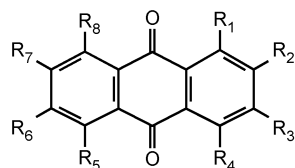
Spectroscopic-grade methanol and ultrapure water (18.2 M Ω \times cm Millipore Milli-Q) were used in the mobile phase. The HPLC mobile phase was degassed by sonication for 1 h prior to use.

RESULTS AND DISCUSSION

The use of the Brewster's angle flow cell CRDS system is demonstrated by static measurements and by coupling to high performance liquid chromatography (HPLC). The baseline ring-down time constant, τ , achieved for pure water in the $300\text{-}\mu\text{m}$

(21) Patel, B. S.; Mallik, A.; Charan S. *J. Phys. E: Sci. Instrum.* **1973**, *6*, 1014–1016.

Table 1. Structures of Anthraquinones



name	R ₁	R ₂	R ₃	R ₄	R ₅	R ₆	R ₇	R ₈
1 alizarin	OH	OH	H	H	H	H	H	H
2 purpurin	OH	OH	H	OH	H	H	H	H
3 quinalizarin	OH	OH	H	H	OH	H	H	OH
4 emodin	OH	H	OH	H	H	CH ₃	H	OH
5 quinizarin	OH	H	H	OH	H	H	H	H

optical path length cell, is 2.5 μs in a 1-m cavity with mirror reflectivities of $R = 0.9993$ at 470 nm. This value decreases over time to $\sim 1.5 \mu\text{s}$ as the surface of the cell is soiled by the poor air quality in the laboratory. Cleaning the outside of the cell with methanol generally returns the baseline τ to its originally aligned value.

Static Measurements. A static calibration curve of quinalizarin was obtained in the HPLC mobile phase (methanol/5% acetic acid in water, 80:20 v/v, pH 3.6) with a minimum detectable concentration of 30 nM at 470 nm (3 σ). The baseline noise of the static system was 2.8×10^{-6} AU rms and 1.0×10^{-5} AU peak-to-peak. The molar extinction coefficient of quinalizarin at this wavelength was $9 \times 10^3 \text{ M}^{-1}\text{cm}^{-1}$, as determined by UV-vis absorbance (and also by CRDS). Concentrations used in the calibration curve ranged from 30 nM to 30 μM , with an R^2 value of 0.9998, giving a linear dynamic range of 3 orders of magnitude. The maximum detectable concentration was determined as one that gave a ring-down time constant of no less than 100 ns. With better detection electronics or a higher baseline τ , the dynamic range could be extended.

Quinalizarin acquired commercially has several impurities that contribute to the absorbance at 470 nm. The contribution of these impurities is negligible below a solution concentration of 1 μM . To remove errors from these impurities at higher concentrations, the solutions used in the calibration curve were run on the HPLC setup to determine the percentage of total absorbance from quinalizarin. For each concentration, the quinalizarin peak area was divided by the total peak area to determine a correction factor, which was then applied to the high concentration static measurements.

HPLC Measurements. For the demonstration of CRDS as an on-line HPLC absorption detector, five compounds belonging to the anthraquinone family (Table 1) were separated and detected as shown in Figure 3.

The compounds are well resolved, with the exception of (2) purpurin and (3) quinalizarin. The lack of baseline resolution between these compounds is partially attributed to an impurity present in the commercially obtained quinalizarin. Additionally, the small peak at ~ 4 min results from another impurity in quinalizarin and is reproducible at higher concentrations.

The baseline noise for the CRDS HPLC detector was 3.2×10^{-6} AU rms and 1.3×10^{-5} AU peak-to-peak. This noise is slightly higher than the static condition and is attributed to solvent flow

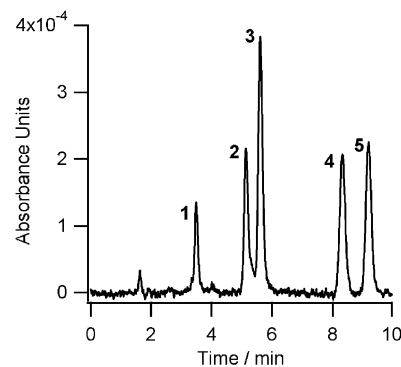


Figure 3. HPLC separation of 10 μM of (1) alizarin, (2) purpurin, (3) quinalizarin, (4) emodin, and (5) quinizarin using CRDS detection in a 300- μm path length cell. The peak shortly before 2 min is the solvent front.

effects. For chromatographic separations, the minimum detectable peak absorbance is taken as twice the peak-to-peak noise, and the corresponding concentration detection limit of quinalizarin is $\sim 0.5 \mu\text{M}$. Peak areas varied by no more than 2–3% for repeated injections of the same concentration. A peak-area calibration curve was obtained for concentrations of quinalizarin, including 0.5, 1, 10, 30, and 50 μM , with an R^2 value of 0.9998, exhibiting a linear dynamic range of 2 orders of magnitude.

The minimum detectable concentration of the HPLC measurements is significantly higher than the minimum detectable concentration for the static measurements. The relatively high dead volume in the flow cell, the extracolumn band dispersion, and the increased noise levels cause this difference. Higher concentrations of quinalizarin could have been detected, but its poor solubility prevented such measurements. Calculations predict the maximum observable concentration of quinalizarin in this HPLC-CRDS system to be at least 0.3 mM, on the basis of an initial τ of 2 μs with the mobile phase and a τ of 100 ns at the peak of the absorber, which corresponds to a dynamic range of close to 3 orders of magnitude, as in the static measurement case.

The same concentration mixture in Figure 3 was run on a commercial instrument (System Gold, Beckman Coulter with model 166NM UV-vis detector) using the same column, injection volume, detection wavelength, and similar mobile phase as the CRDS setup, but with a 10-mm path length cell. The commercial instrument uses a stable deuterium lamp as the light source (filters are used to achieve a 470 nm detection wavelength) and matched photodiodes as the detector. Figure 4 shows the separation.

The peak areas for the separation detected by standard UV-vis absorption are 33.3 times larger than the peak areas for the separation detected by CRDS for the same concentration. This difference is attributed entirely to the difference in path length, as expected. The slight difference in peak heights between the CRDS and commercial measurements of peaks 4 and 5 is most likely due to the broader spectral bandwidth (5 nm) of the commercial instrument. The other peaks have a fairly flat absorption profile between 467 and 473 nm.

To simulate the effect of a shorter path length cell, concentrations that were 33.3 times smaller (0.3 μM , as compared with 10 μM) than those run on the CRDS setup were separated and detected by the commercial instrument. The raw data was then subjected to an 11-point boxcar average for better comparison with

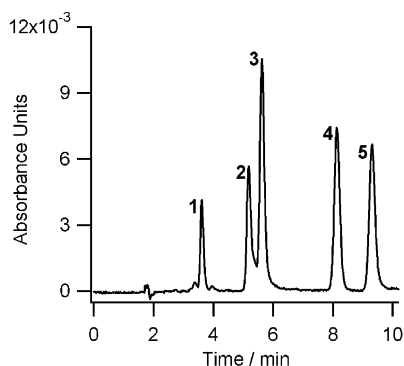


Figure 4. HPLC separation of 10 μM of (1) alizarin, (2) purpurin, (3) quinalizarin, (4) emodin, and (5) quinizarin using standard UV–vis detection in a 10-mm path length cell. The peak shortly before 2 min is the solvent front.

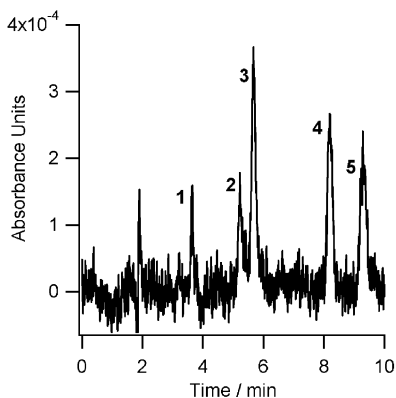


Figure 5. HPLC separation of 0.3 μM of (1) alizarin, (2) purpurin, (3) quinalizarin, (4) emodin, and (5) quinizarin using standard UV–vis detection in a 10-mm path length cell. The peak shortly before 2 min is the solvent front.

the CRDS system. This separation, after averaging, is shown in Figure 5.

The peak-to-peak baseline noise for this power-fluctuation-subtracted UV–vis detector is specified to be 2×10^{-5} AU peak-to-peak, but even after averaging, it is measured at 1×10^{-4} AU peak-to-peak in the present instrument. The rms baseline noise is 2.2×10^{-5} AU. Comparison of Figures 3 and 5 suggests that the CRDS detection system is superior to this particular instrument.

Comparison with Standard UV–Vis Detectors. For a small absorption coefficient, a first-order Taylor expansion can be applied to the expression $I = I_0 e^{-\alpha l}$ and the definition for absorbance can be written as

$$\text{AU} = \left(\frac{1}{2.303} \right) \left(\frac{\Delta I}{I} \right) \quad (4)$$

For comparison with standard absorption detection, eq 2 for CRDS can be rewritten

$$\text{AU} = \frac{t_r}{2(2.303)\tau} \left(\frac{\Delta\tau}{\tau} \right) \quad (5)$$

The benefit of using CRDS is that for an equivalent per-pass absorption coefficient, there is a greater difference in values

between the variables being measured. For example, the measurement of 1×10^{-4} AU requires $\Delta I/I$ to be 2.3×10^{-4} , or 0.023%, whereas for CRDS, $\Delta\tau/\tau$ is 14% for a 1-m cavity with τ_0 of 2 μs . The current minimum detectable AU for standard single-pass absorption spectroscopy is 1×10^{-5} . This value means $\Delta I/I$ must be determined to within 0.0023%, whereas for CRDS, $\Delta\tau/\tau$ need be determined only to within 1.4%.

Theoretically, if $\Delta\tau/\tau$ could be measured to the same degree that $\Delta I/I$ can be, then the minimum detectable absorbance would be 1.7×10^{-8} AU for a 1-m cavity with τ_0 of 2 μs . However, unlike for standard absorption spectroscopy, $\Delta\tau/\tau$ is limited only in the best case by how well τ and τ_0 can be measured. The uncertainty determined from fitting a single curve should be the same as the ensemble $\sigma_\tau/\bar{\tau}$ only if the shot-to-shot fluctuations in τ are a result of statistical errors rather than systematic errors.²² This ideal behavior is not attained in most pulsed CRDS systems. The limitation comes from the fact that a pulsed laser has a broad line width that couples to many available cavity modes, leading to mode-beating and multiexponential decays. Additionally, if the cavity is not length-stabilized, the cavity modes vary from shot to shot. A detailed discussion of mode behavior is beyond the scope of this paper. The interested reader is directed to several papers discussing the intricacies of cavity ring-down spectroscopy.^{5,23,24} Let it suffice to say that with a pulsed system exhibiting multimode behavior and a nonlength-stabilized cavity, $\sigma_\tau/\bar{\tau}$ is typically $\sim 1\%$ shot-to-shot. A significant improvement in the value for $\sigma_\tau/\bar{\tau}$ can be obtained by simply changing to a single-mode laser source. van Zee et al.²⁵ describe the use of a frequency-stabilized, single-mode pulsed laser in conjunction with a length-stabilized cavity to achieve a $\sigma_\tau/\bar{\tau}$ of 0.03%. Additionally, Crosson et al.²⁶ describe the use of a continuous-wave single-mode laser source that is coupled to a ring-down cavity by sweeping the cavity length to achieve a $\sigma_\tau/\bar{\tau}$ of 0.03%, as well.

Our results illustrate that a simple pulsed CRDS system with little effort put into mode matching or cavity stabilization provides a minimum detectable absorbance that is roughly equivalent to, if not slightly better than, the best available commercial detectors. Any improvement made to the cavity ring-down system, such as operating at a higher pulse repetition rate or using a single-mode light source, will result in increased sensitivity over that currently available.

CONCLUDING REMARKS

We describe the application of cavity ring-down spectroscopy (CRDS) to the liquid phase via implementation of a Brewster's angle flow cell and its subsequent use as an on-line chromatographic detector. Using a relatively simple CRDS setup, we achieve a performance that is equivalent to or better than a high-quality commercial UV–vis absorption system. By decreasing the value of $\sigma_\tau/\bar{\tau}$, this CRDS technique is expected to surpass significantly standard absorption detectors.

(22) Bevington, P. R.; Robinson, D. K. *Data Reduction and Error Analysis for the Physical Sciences*; McGraw-Hill: New York, 1992.

(23) Lehmann, K. K.; Romanini, D. *J. Chem. Phys.* **1996**, *105*, 10263–10277.

(24) Hodges, J. T.; Looney, J. P.; van Zee, R. D. *J. Chem. Phys.* **1996**, *105*, 10278–10288.

(25) van Zee, R. D.; Hodges, J. T.; Looney, J. P. *Appl. Opt.* **1999**, *38*, 3951–3960.

(26) Crosson, E. R.; Ricci, K. N.; Richman, B. A.; Chilese, F. C.; Owano, T. G.; Provencal, R. A.; Todd, M. W.; Glasser, J.; Kachanov, A. A.; Paldus, B. A.; Spence, T. G.; Zare, R. N. *Anal. Chem.* **2002**, *74*, 2003–2007.

The Brewster's angle flow cell–CRDS system is simple to align and operate. Once aligned, no adjustments are needed for an extended period of time. The design of the flow cell can be modified to accompany volumes suitable for micro-HPLC and possibly capillary electrophoresis (CE). In applying CRDS to nanoliter-volume systems, it is necessary to focus the beam through an aperture that is generally $<100\ \mu\text{m}$. To avoid diffraction losses and, thus, a reduction in the ring-down time constant, the Gaussian beam waist should be at least 4.6 times smaller than the aperture, a condition discussed by Siegman²⁷ and verified experimentally by Zhao et al.²⁸ Such a tightly focused beam in a stable resonator is difficult to achieve because confocal or near-confocal geometry is required. The application of CRDS to nanoliter-volume systems is an area of interest because detection

limits for these low-volume techniques are comparatively quite high, owing to the short path length of capillaries. Efforts to increase the capillary path length, for example, the creation of bubbles or z-cells, result in a reduction of efficiency and resolution.²⁹ Some success with multireflection capillaries has been reported,³⁰ but these devices suffer from a loss in efficiency and are difficult to reproduce. The implementation of such a miniaturized system remains a challenge for future work.

ACKNOWLEDGMENT

The authors thank Hellma Cells, Inc. for their help in designing and building the flow cell and the Stanford Physics Machine shop for building the flow cell mount. We are grateful to Eric Pesle at Spectra Physics for his unfailing assistance with the laser. We thank Christopher Amos and Tom Wandless at Stanford University for use of the commercial HPLC instrument. K.L.S. is currently on an Evelyn Laing McBain fellowship. This work has been funded by ONR Grant no. N000140010364.

Received for review January 7, 2003. Accepted April 6, 2003.

AC0340152

(27) Siegman, A. E. *Lasers*; University Science Books: Sausalito, CA, 1986; Chapter 19.

(28) Zhao, M.; Wahl, E. H.; Owano, T. G.; Largent, C. C.; Zare, R. N.; Kruger, C. H. *Chem. Phys. Lett.* **2000**, *318*, 555–560.

(29) Xue, Y.; Yeung, E. S. *Anal. Chem.* **1994**, *66*, 3575–3580.

(30) Wang, T.; Aiken, J. H.; Huie, C. W.; Hartwick, R. A. *Anal. Chem.* **1991**, *63*, 1372–1376.